Using triaxial magnetic fields to create high susceptibility particle composites

James E. Martin, Eugene Venturini, Gerald L. Gulley,* and Jonathan Williamson

Sandia National Laboratories, Albuquerque, New Mexico 87185-1421, USA

We report on the use of triaxial magnetic fields to create a variety of isotropic and anisotropic magnetic particle/polymer composites with significantly enhanced magnetic susceptibilities. A triaxial field is a superposition of three orthogonal ac magnetic fields, each generated by a Helmholtz coil in series resonance with a tunable capacitor bank. Field frequencies are in the range of 150–400 Hz. Because both the field amplitudes and frequencies can be varied, a rich variety of structures can be created. Perhaps the most unusual effects occur when either two or three of the field components are heterodyned to give beat frequencies on the order of 1 Hz. This leads to a striking particle dynamics that evolves into surprising structures during resin gelation. These structures are found to have perhaps the highest susceptibility that a particle composite can have. The susceptibility anisotropy of these composites can be controlled over a wide range by judicious adjustment of the relative field amplitudes. These experimental data are supported by large-scale Brownian dynamics simulations of the complex many-body interactions that occur in triaxial magnetic fields. These simulations show that athermal three-dimensional field heterodyning leads to structures with a susceptibility that is as high as that achieved with thermal annealing. Thus with coherent particle motions we can achieve magnetostatic energies that are quite close to the ground state.

INTRODUCTION

Motivation

In a recent paper [1] it has been shown that uniaxial or biaxial (e.g., rotating) magnetic fields can be used to create structured magnetic particle-polymer composites with enhanced magnetic properties along the direction of the structuring field. Relative to a random particle composite, the susceptibility of uniaxial field-structured composites (FSC's) is enhanced along one principal direction, and suppressed along the other two, and the converse holds for biaxial FSC's. In this paper it was shown through a mean-field theory that the sum of the inverse magnetic susceptibilities along three principal directions is invariant to structuring, so that enhancements must be balanced by suppressions. This invariant was demonstrated in experiments on a variety of composites containing carbonyl iron particles. The existence of this invariant implies that it is not possible to organize the particles in such a way as to enhance the susceptibility of an FSC along all three principal directions.

In fact, we have recently shown through theory and simulation that triaxial magnetic fields *can* be used to create particle composites with significant susceptibility enhancements in all three principal directions [2]. Triaxial FSC's violate the inverse susceptibility sum rule because of large local-field fluctuations that render a mean-field approximation inaccurate. The purpose of this paper is to demonstrate significant susceptibility enhancements in isotropic FSC's experimentally, and to explore how triaxial magnetic fields can also be used to create optimized anisotropic composites. Particle interactions in triaxial magnetic fields are strange, and some discussion of this will help to motivate this paper.

Interactions in a triaxial field

When a random suspension of magnetically soft particles is exposed to a uniaxial magnetic field, dipoles are induced that are closely aligned with the applied field. The particles will move under the influence of the dipolar interactions with nearby particles in such a fashion as to increase their dipole moments, forming complex chainlike structures that reduce the suspension magnetostatic energy. We call interactions in a uniaxial field *positive* dipolar interactions. These interactions are invariant to inversion of the field, since this merely inverts the sign of each dipole and the interactions depend on the square of the dipole moment. A *negative* dipolar interaction between two particles can in principal be created by inverting the field at only one of the dipoles, but this is impractical, and in any case it would not be possible to create negative dipole interactions between all particles with such an approach.

It is possible to create a time-average *negative* dipole interaction between particles by subjecting the suspension to a rapidly changing biaxial (e.g., rotating) magnetic field in a plane normal to the uniaxial field described above. The induced dipole moments create a net average attractive interaction in the plane of the field, resulting in the formation of complex sheetlike structures [3]. A simple first-order calculation [4] shows that the average interaction is just the opposite of a positive dipolar interaction, so that in a balanced triaxial field, where both the uniaxial and biaxial fields are applied simultaneously (and with all three field components having equal rms amplitudes), one might expect no interaction at all. Experiments show that this is not the case, and an exact point dipole calculation shows that the negative dipolar interactions created by a biaxial field are not exactly equal and opposite to the positive dipolar interactions.

This lack of perfect symmetry between interactions in uniaxial and biaxial fields is due to the fact that the particles

---

*On leave from Dominican University, Dept. of Natural Science, River Forest, IL 60305.

magnetize in the local field, not the bare applied field, which can be viewed as a sum of the macroscopic field and the microscopic field. The smooth macroscopic field is the sum of the applied field plus the Lorentz cavity field (provided demagnetizing fields due to the sample shape can be eliminated). The lumpy microscopic field is due to the nearby dipoles. Each dipole moment thus has parts due to the macroscopic and microscopic fields. It can be shown that in a balanced triaxial field the part of the moments due to the macroscopic field leads to zero average interaction, but the part due to the microscopic field leads to strong and complex many-body interactions. Complex because the interaction between three contacting particles cannot even be approximately described by the sum of the pair potential. Because of this all of the usual things one might expect of an isotropic system with attractive interactions, such as the formation of periodic lattices, fail to occur. Instead, particle structures with molecularlike geometries are stable, and at equilibrium a suspension forms a particle foam [2].

By the judicious selection of field component amplitudes and frequencies, a rich variety of FSC's can be formed in triaxial magnetic fields. If all three field frequencies are widely separated a particle gel forms, Fig. 1 (top). If two of the field component frequencies are sufficiently close together that the particles can follow the beat frequency, then a striking oscillation occurs, which we call 2-d heterodyning, that leads to the formation of a honeycomb structure, Fig. 1 (center). If all three component frequencies are close, a complex collective dynamics occurs, which we call 3-d heterodyning, that leads to a particle foam, Fig. 1 (bottom). Heterodyne structures are found to have highly optimized properties. To create structures with anisotropic magnetic properties the rms field amplitudes can be imbalanced. In this paper we consider both positive and negative uniaxial biases, which lead to composites with enhanced susceptibilities along one or two principal directions, respectively.

Optimizing the magnetic susceptibility also optimizes isomorphic properties, such as the dielectric constant and thermal and electrical conductivity (not quite isomorphic, but still optimized). Thus we believe that this new class of triaxial field-structured composites (FSC's) hold great promise as practical materials for many applications [5].

Background

Although this is a report of the magnetic properties of particle composites structured by triaxial fields, there have been several other studies of the magnetic properties of materials structured into chains by a uniaxial field. O'Grady *et al.* [6] created two different ferrofluids by the thermolysis of di-cobalt octacarbonyl in toluene, controlling the particle size by appropriate surfactant selection. This resulted in a superparamagnetic particle sample of 5.0-nm particles, and a ferromagnetic sample of 12.0-nm particles. These nanoparticles apparently consisted of essentially single crystalline domains, so that texture could be introduced into the samples by particle alignment. In the superparamagnetic sample a significant increase in the susceptibility was found when the samples were field cooled, which oriented the particles in the
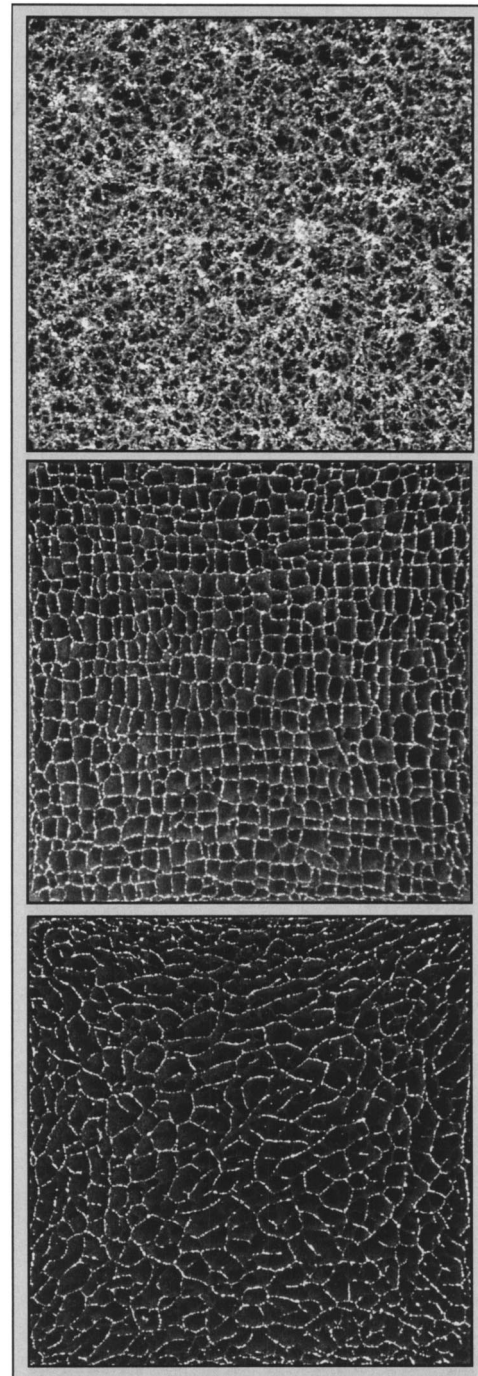
FIG. 1. Sample structures made in triaxial magnetic fields. In a triaxial field a particle gel forms (top). In 2-d heterodyning a honeycomb structure forms (center). 3-d heterodyning leads to a particle foam (bottom). These composites were made with large, 50-μ Ni particles to facilitate optical imaging. The incident light images are 1 cm across.

frozen solvent, leading to significant texture, since each particle consists of essentially a single crystalline domain. In the ferromagnetic particle sample a significant increase in the remanence was observed in a field-cooled sample, again due to particle rotation along an easy axis creating significant texture. An analysis in terms of texture is given, but it is not

clear if the particles formed chains, though at least the larger particles certainly should have. Brugel *et al.* [7] made platelets by ball milling a thin film of Metglas 2605SC. The platelets were oriented in a magnetic field of 0.4 T, due to the relatively small demagnetizing field in the plane of the platelets, and the polymer resin was then cured. Shifts in the magnetization curves of these materials were found which they attributed to particle alignment, though it is possible that the observed shifts were partly due to the strong local fields produced by particle chains. Jin *et al.* [8,9] have investigated uniaxial FSC's of 20 and 75-μm Ni particles coated with a thin layer of Ag. The conductivity of these materials in response to applied strains was the principal goal, but some magnetization measurements were reported that indicated that these materials have isotropic magnetic properties. This is not what we find for uniaxial FSC's, but perhaps their assessment was intended to be qualitative.

Studies of the magnetic properties of sheetlike particle aggregates, such as those that form in rotating fields, are apparently limited to Fabre *et al.* [10], who created a "Smectic Ferrofluid"—sheets of superparamagnetic maghemite particles—by swelling a lamellar micelle solution of the surfactant/cosurfactant system sodium dodecyl sulfate/pentanol with nanosize maghemite in cyclohexane to form a lamellar microemulsion. Due to the dependence of demagnetizing factors on lamellar orientation, these fluid phases orient in modest fields (100 G), so that the magnetic field is parallel to the lamallae. Measurements of the magnetization of these phases was not reported, though one would expect a large difference between cooled and field-cooled samples, if the matrix could be frozen without upsetting the phase stability of the microemulsion.

Creating optimal particle composites

The goal of this paper is to use triaxial magnetic fields to substantially improve the susceptibility of isotropic and anisotropic particle composites. That this is possible with triaxial fields is an issue that merits some discussion.

Uniaxial fields

Consider first the much simpler problem of optimizing the susceptibility of a particle composite along a single direction. Tao and Sun [11] showed that the magnetic ground state of such a system occurs when the particles are packed into a body-centered-tetragonal (bct) lattice, with the unique axis aligned with the applied field. In this configuration it is shown as follows that the composite susceptibility will be optimized in the direction of the structuring field. In mks units the energy of an induced dipole in an applied field $\mathbf{H}_0$ is $U = -\frac{1}{2}\mu_0 \mathbf{m} \cdot \mathbf{H}_0$, where $\mathbf{m}$ is the dipole moment of each particle and is proportional to the local field. The sample magnetization $\mathbf{M}$ is the dipole density, $\mathbf{M} = \phi \mathbf{m}/v$, where ϕ is the particle volume fraction and v is the dipole volume. The composite susceptibility is the magnetization per unit field, which, noting that the moments are parallel to the field, can be expressed as $\chi = \phi u_{\text{dipole}}/u_{\text{field}}$ where the energy density of each dipole is $u_{\text{dipole}} = U/v$ and the energy density of

the field is $u_{\text{field}} = -\frac{1}{2}H_0 B_0$. Thus minimizing the energy of a dipole maximizes the susceptibility.

The magnetophoretic force on a particle is in the direction of the gradient of that component of the local field which is parallel to the particle moment. Thus in the absence of thermal fluctuations each particle will move to increase its moment, enhancing the composite susceptibility. Brownian dynamics simulations of suspensions of spherical particles do show a progression to the bct structure, with a concomitant increase in the susceptibility [12].

The experimental situation is more complex for three reasons: particle roughness creates strong local minima, shape and size polydispersity eliminate the possibility of lattice formation, and Brownian forces are negligible compared to gravitational forces. Because of the latter, it is not possible to reduce the field to the point where dipolar forces are comparable to Brownian forces, as the suspension will simply sediment. Real composites made in a uniaxial field thus exhibit quenched disorder. One could certainly make composites of density-matched magnetic particles, such as polystyrene lattices filled with magnetite particles, but the particle susceptibility is then too small for strong collective magnetic effects to emerge. The same is true for density-matched systems created by coating a nonmagnetic particle with magnetic material. Even so, susceptibility enhancements of 2.5 have been achieved for uniaxial FSC's.

Triaxial fields

In a triaxial magnetic field the particles will move to increase the composite susceptibility along all three directions, thus maximizing the susceptibility sum. As shown in the discussion of heterodyning below, this is because the force on each particle is a simple sum of the forces due to each field, corresponding to the incoherent interaction of dipole moments. The same result could be obtained by applying consecutive field pulses along the *x, y, z* directions.

In our previous paper we computed the susceptibility of a variety of simple structures, finding that a sheet of particles, or a bilayer, had by far the highest susceptibility sum (over three principal directions) of any structure considered. However, athermal triaxial field simulations gave disappointing results, because the particles tended to form a network of chains with only modest susceptibility enhancements. Thermal simulations gave much improved results, showing the formation of a high susceptibility particle foam structure. This particle foam consists of monolayer particle sheets, and can be thought of as a way of embedding a sheet into three dimensions. But this result does not lead us to a prescription for synthesizing optimal composites, because thermal fluctuations are negligible in our system.

The important finding in our previous paper is that simulations of heterodyned triaxial fields can lead to composite structures with very high susceptibilities, even in the absence of thermal fluctuations. This then is indeed a prescription for the synthesis of real optimal composite materials. The details of heterodyning are given below, but the basic idea is that the slow beating of field components causes an oscillation between the coherent and incoherent interaction of the dipole moments induced by the three field components. This leads

to a complex periodic motion of particle sheets in the suspension. As the polymer resin gels, its viscosity diverges continuously, until the sheets can no longer follow the field beats. In this stage surprising structures emerge, both in simulation and experiment. In particular, if all three field components are heterodyned, the emergent structure closely resembles that arising from simulated annealing, indicating that this technique can mimic the effect of Brownian motion.

In this paper we first describe the synthesis and characterization of these materials, and the simulation method we have developed. This is followed by a discussion of heterodyning, a report on our experimental and simulation results, and the development of simple analytical expressions for the susceptibility of the structures we observe.

EXPERIMENT

Sample preparation

A 4–7-μm Ni powder from Goodfellow™ was used to make all composites for magnetic susceptibility measurements, with concentrations in the range of 0.1–30.0 vol %. The particles were suspended in a polyester resin (Castin' Craft™ liquid polymer casting resin) without the use of a dispersant. After addition of the catalyst, these suspensions were degassed in a vacuum chamber for 3 min, and poured into 1-cm square polystyrene cuvettes. Each cuvette was filled to a height of 1 cm to insure that the demagnetizing fields are the same in all directions (of course, this is not true for the anisotropic samples, but in this case it is not so important either). The samples were then structured in the triaxial magnetic field until well past the gel point (25 min) and post-cured in an oven at 70 °C for at least 2 h. These samples were then accurately machined into 4.00-mm cubes for susceptibility measurements. A cube was chosen because we have developed an accurate way to correct for the demagnetizing fields for this shape (below).

To create a uniform triaxial magnetic field we constructed three nested orthogonal Helmholtz coil pairs. Although all three fields are equivalent, it is useful in much that follows to think of one component as the uniaxial field and the other two as forming a biaxial field. The uniaxial field either is run dc with a current source or is driven ac with a fixed capacitor in series to create a series resonance at 203.7 Hz with an impedance of ≈ 2.6 Ω. The biaxial field components are run ac and are connected to tunable, computer-controlled, series-parallel capacitor banks of our own design to create series LRC circuits with high quality factors and a resonant impedance of ≈ 2.2 Ω. The capacitor banks use high quality Silicon-Controlled Rectifier capacitors from General Electric which have high current and voltage specifications and low stray inductance. The banks use 12 capacitors each, spanning from 1 to 100 μF, and have $\sim 354\,000$ capacitance values spanning three decades of capacitance, easily enough to create series resonance at selected coil frequencies from ≈ 125–1500 Hz. Potter and Brumfield power relays with a 4-kV standoff are used to switch the capacitors and the 24-V switching voltage is supplied through a control board based on 4-kV standoff optical isolation relays. These relays are driven by logic pulses from a 96 channel I/O board from

National Instruments installed in a Power Macintosh and are controlled by a Labview program. Extremely accurate calibration of the capacitors is essential, and was accomplished with an Agilent 4284A LCR bridge. Driving these circuits with an ATI model 1504 audio power amplifier with 200 W per channel it is possible to create magnetic induction fields as large as 500 G at frequencies up to ≈ 1500 Hz in the smallest coil. Amplifier input signals are provided by a phase-locked Multifunction Synthesizer from Agilent, model 8904A [13]. During operation, extremely high voltages appear across the coil and capacitors, so due regard for safety must be exercised, mostly through the use of electrical insulation and safety interlocks.

In some experiments one of the field components was amplitude modulated. In practice this was the largest coil because this has the lowest quality factor at any given operating frequency. The reasonably wide resonance makes it possible to drive this coil effectively with a signal that is the sum of two frequencies as much as a few Hz apart, causing amplitude modulation at the beat frequency of the two signals. Amplitude modulation should not be confused with our use of the term heterodyning, by which we refer to the beating of one field component against another.

Magnetic measurements

Isothermal magnetic hysteresis data were measured at room temperature (295 K) for applied fields between +1 and −1 T using a commercial superconducting quantum interference device (SQUID) magnetometer with extended dynamic range (200 emu). The extended range allowed the use of relatively large samples (typically $4.00 \times 4.00 \times 4.00$ mm^3) with saturation moments up to 10 mA m^2 (10 emu) for 30 vol % Ni. These dimensions are much larger than the coarseness of the composites, assuring a representative result. At the maximum field of 1 T these samples were in the reversible approach-to-saturation regime, minimizing any history effects in the measurements. The susceptibilities reported herein were taken from the slope of the magnetization curve at zero moment for a partial hysteresis loop starting from near saturation.

Correcting for demagnetizing fields

Because the samples were machined into cubes it was necessary to correct the susceptibility data for demagnetizing fields. To do this we simulated a cubic lattice of dipoles occupying a cubical volume. A 3-d finite difference code was written to solve the applicable Maxwell equation $\nabla \cdot \mathbf{B} = \nabla \cdot \{[1 + \chi(\mathbf{r})]\mu_0 \mathbf{H}(\mathbf{r})\} = 0$ iteratively, and thereby determine the macroscopic field, for a cube of a continuum soft ferromagnet of relative magnetic permeability μ_r placed in an initially uniform magnetic field [1]. We used a Cartesian mesh of magnetostatic potentials to represent the cube of permeable material and a substantially larger volume of $\mu_r = 1$ space surrounding it. The mesh surfaces were set to constant potential or constant electric field, as appropriate, which is equivalent to immersing the central cube in an infinite 3-d lattice of its images. These boundary conditions caused minimal perturbation because a simple cubic lattice

of identical dipoles produces zero field at a lattice site. The cubic symmetry provided the additional advantage of allowing the computation to be restricted to one-eighth of the total volume. Results were obtained for several choices of mesh coarseness and were extrapolated to an infinitely fine mesh. A second extrapolation to zero cube size (relative to the full computational mesh) gave the final result for the macroscopic field inside the cube.

Because the cube is nonellipsoidal, the macroscopic field $\mathbf{H}_{macro}$ within the cube is not uniform and not generally parallel to the applied field, taken to be along the z axis. A demagnetization factor was therefore defined by averaging the component of the computed macroscopic field along the initial field, $n = [H_0 - \langle \mathbf{H}_{macro} \cdot \hat{\mathbf{z}} \rangle] / \chi \langle \mathbf{H}_{macro} \cdot \hat{\mathbf{z}} \rangle$. The demagnetization factor depends on χ for such a nonellipsoidal shape. The computation was repeated for a range of χ and it was found that the Padé approximate $n = 0.274\,40 + 0.147\,35/(\chi + 2.5486)$ fit the data extremely well. The measured susceptibility χ_m of a cube is related to the true susceptibility χ by $\chi = \chi_m / [1 - n(\chi)\chi_m]$ and the data are corrected self-consistently by iterating this expression with the Padé for n, convergence taking only a few iterations. As a check on the Pade, simulations were done by relaxing a cubic lattice of induced dipoles with a selected value of the susceptibility [14], using the Clausius-Mossotti equation [15] to relate the magnetizability per unit volume to the bulk susceptibility. Extrapolation to an infinite number of dipoles yielded a demagnetization factor in excellent agreement with the Padé.

SIMULATION METHOD

We have reported athermal [1,16] and thermal [12] simulation studies of structure formation in uniaxial and biaxial field-structured composites, but these simulations were based on the fixed point dipole approximation (i.e., magnetization in the applied field), which would give zero interactions in a triaxial field. A new simulation was written to compute interactions in a triaxial field. This simulation is exact in the self-consistent point dipole approximation, the primary difference being the consideration of the microscopic field in the computation of the dipole moments. In addition, other aspects of the simulation were modified to create a robust, stable code.

In this Brownian dynamics simulation the particles are essentially hard spheres with induced dipolar interactions, Stokes friction against the solvent, and Brownian motion. The essentially hard spheres have an interaction force that increases as the sixth power of their *overlap*, specifically, $f \propto (1.03d - \Delta r)^6$ for $\Delta r < 1.03d$, where d is the particle diameter and Δr is the separation distance between the centers of masses of the particles. Note that "overlap" starts when there is actually a 3% gap between the particles. The hard force amplitude can be chosen in a number of ways, but we chose it such that two particles in a balanced triaxial field of unit rms component amplitudes would have a center-of-mass separation equal to d. Larger agglomerates, such as a chain of particles, will compress somewhat, an issue to which we will return.

To compute dipole interactions exactly in the point dipole approximation one must take into account that the field that magnetizes the dipoles is the local field, which is the applied field plus the field due to the other dipoles. In addition, the magnetization of a single isolated particle is actually affected by the field created by its magnetization [17], limiting the susceptibility (mks units) of a spherical particle to $\chi = 3\beta$, where $\beta = (\chi_p - \chi_l)/(3 + \chi_p + 2\chi_l)$ in terms of the intrinsic susceptibilities χ_p and χ_l of the materials of which the particle and liquid phases are composed. For magnetic particles, β can be as large as 1; for magnetic holes, as small as $-\frac{1}{2}$. The moment of a particle of volume v can then be written in terms of the local field as $\mathbf{m} = 3\beta v \mathbf{H}_{local}$, and the force on a dipole is $\mathbf{F} = \mu_0 \mathbf{m} \cdot (\nabla \mathbf{H}_{local})$. In a nonheterodyned triaxial field we have shown that it is only necessary to sum the force for fields applied along three orthogonal axes [2].

The computation of the local field is a subject about which there is a certain degree of confusion in the literature [14]. We use the method of Lorentz (not to be confused with the Lorentz approximation), which enables the errors in the local field to be made as small as desired. We do not use Ewald sums, an alternative method. Our simulation volume is a cube with cyclic boundary conditions.

The macroscopic field at each dipole is taken to be the applied field plus the Lorentz cavity field, which is exactly $\mathbf{M}/3$ for the spherical cavity we employ (see below), with $\mathbf{M}$ the sample magnetization. The demagnetizing field due to the overall shape of the simulation volume is zero because when we compute the field at each dipole the simulation volume is always taken to be centered on that dipole, which is another way of using the cyclic boundary conditions, in addition to particle reentry.

The microscopic field at each particle is computed by summing the dipole fields $\mathbf{H}_m = (1/4\pi r^3)[3(\mathbf{m} \cdot \hat{\mathbf{r}})\hat{\mathbf{r}} - \mathbf{m}]$ from all the particles within a spherical cavity with a diameter that in practice is not less than $10\times$ the particle diameter. Here $\hat{\mathbf{r}}$ is the unit vector from the particle center of mass. These nearby dipoles are computed with an efficient neighbors algorithm used in our previous simulations. The sum of the microscopic field and the Lorentz cavity field is the total field from all the dipoles and their images. Errors can result from this approach if the cavity size is smaller than the characteristic internal scale of the structure. In practice this method is sufficiently precise that when we calculate the sample magnetization by enlarging the spherical cavity to include the entire simulation volume, the magnetization changes by $\approx 1.0\%$. Finally, local update is used in the calculation of the dipole moments because we found that global update could result in oscillation instabilities.

One critical numerical issue arises because a system of soft magnetic particles is perilously close to spontaneous magnetization. We have shown above that the susceptibility of a typical soft magnetic particle is quite close to 3. A straightforward calculation shows that a long chain of contacting particles will magnetize spontaneously if the particle susceptibility is $6/\zeta(3) \approx 5$, where $\zeta(x)$ is the Riemann zeta function. If the chain is slightly compressed to force the particles to overlap, spontaneous magnetization will occur at a

center-of-mass separation of $d[\zeta(3)/2]^{1/3} \approx 0.844d$, at which point the dipolar force is infinite. Because of the proximity of this force divergence it is easily possible to choose a ''hard'' sphere potential that is insufficiently stiff to prevent an agglomerate from collapsing to a point. There are two ways around this problem. First, one can choose an extremely stiff hard sphere potential. This is a poor solution because it leads to force gradients that are extremely large, necessitating unreasonably small time steps for the particle dynamics to remain stable. Second, one can simply limit the dipole force *and* dipole field from overlapping particles to that which would obtain if the particles were exactly in contact. This approach eliminates black hole formation and enables the use of a hard sphere potential that does not generate terrific force gradients, permitting a long time step.

The final simulation issue is stability. Our code is stabilized by keeping track of the force gradients and limiting the time step in proportion to the inverse gradient. In practice, during a simulation cycle each particle is locally advanced through the entire time interval, but this time interval is subdivided into smaller time steps if the program determines that the force gradients are unacceptably large. This is very effective in reducing execution time and allows the code to make 10 000 particle runs on a Macintosh G4 in a reasonable amount of time. Subdividing the time step is especially effective because of the way in which we move the particles. Typically one computes the total force on a particle (interacting with perhaps 500–1000 neighbors) and moves it. We compute the interaction between each pair of particles and move just that pair immediately. The advantage of doing this is twofold. First, the center of mass of the system is strictly preserved. Second, large force gradients only occur between contacting particles, so when a time step is subdivided, the 500–1000 interactions do not need to be recomputed. There are typically six contacting interactions, so the time savings is substantial. Because of these considerations the code is remarkably stable: For example, compressing a chain of spheres to 50% overlap gives forces that are $\approx 10^{10}$ times that expected in the simulation. This causes no problem at all, the chain simply expands back to its equilibrium length.

Timescale

The athermal equation of motion is obtained by balancing the dipolar force, against the hydrodynamic drag force $\mathbf{F}_{\text{hydro}} = -6\pi\eta a\mathbf{v}$, where a is the particle radius, η is the liquid viscosity, and $\mathbf{v}$ is the particle velocity. The many-body dipolar force cannot be written in closed form, but is of the form $\mathbf{F}_{\text{dip}} = a^2\mu_r\mu_0 H_0^2\mathbf{f}_{\text{dip}}$, where $\mu_0 = 4\pi\times10^{-7}$ Wb/(A m) is the vacuum permeability, μ_r is the relative permeability of the liquid phase, H_0^2 is the mean-square field amplitude, and $\mathbf{f}_{\text{dip}}$ is a dimensionless force. This results in a dimensionless equation of the form $\Delta u = \Delta s f(r,\theta)$, where the dimensionless length $u = r/2a$ and the dimensionless time is $s = t/\tau$ with $\tau = 12\pi\eta/\mu_0 H_0^2$. For a nonmagnetic suspending liquid with a viscosity η_0 of 1 cp, this characteristic time τ is 1 ms with an applied field of $H_0 = 5.5\times10^3$ A/m (69 Oe). The simulation data we generate are for structures that have evolved for 100 dimensionless time units or less.

Brownian motion

The magnitude of the Brownian force is set by the parameter $\lambda = \pi a^3\mu_r\mu_0 H_0^2/k_B T$. In most of the thermal anneals reported here, we start with $\lambda = 2.67$, anneal for 20 dimensionless time units, then linearly ramp temperature (i.e., $1/\lambda$) down to zero in five dimensionless time units. In some of the anneals we start at the same temperature but linearly ramp to zero over 25 time units. For 10 000 particles this takes a little less than 3 days on a 1-GHz Macintosh G4. Heterodyned simulations were athermal and took 12 days to achieve 100 dimensionless time units. The simulation data reported here represent ≈ 225 days of CPU time.

HETERODYNING

Heterodyning is an important experimental technique, and is used in our simulations, so a detailed discussion of this is necessary. In our previous paper we discussed the issue of particle *energies* in 2-d heterodyning but here we describe the particle *forces* in both 2-d and 3-d heterodyning. We start by addressing the issue of dipole interactions in time-dependent fields. A particle of moment $\mathbf{m}_i$ is magnetized by the local field $\mathbf{H}_{\text{loc}} = \mathbf{H}_0 + \Sigma_{k\neq i}\mathbf{H}_{i,k}$, where $\mathbf{H}_{i,k} = (1/4\pi r_{ik}^3)[3(\mathbf{m}_k\cdot\hat{\mathbf{r}}_{ik})\hat{\mathbf{r}}_{ik} - \mathbf{m}_k]$ is the field at the ith particle due to the kth dipole. The force on this dipole is $\mathbf{F}_i = \mu_0\mathbf{m}_i\cdot(\nabla\mathbf{H}_{\text{local}})$, which can thus be written as a sum of contributions, $\mathbf{F}_i = \mu_0\mathbf{m}_i\cdot\Sigma_{k\neq i}\nabla\mathbf{H}_{ik}(\mathbf{m}_k,\mathbf{r}_{ik})$. Each contribution f_{ik} to the force is a linear function of the moments, so $\mathbf{F}_i = \Sigma_{k\neq i}f(\mathbf{m}_i,\mathbf{m}_k)$ where $f(\lambda\mathbf{m}_i,\gamma\mathbf{m}_k) = \lambda\gamma f(\mathbf{m}_i,\mathbf{m}_k)$. To understand heterodyning we need only consider the contribution to the total force from any one pair of particles in a particle agglomerate, which should not be taken to mean that interactions in the agglomerate can be described by summing a pair potential!

Coherence

For simplicity we start with a rotating field in the *x-y* plane, $\mathbf{H}_0 = H_0[\cos(\omega t)\hat{\mathbf{x}} + \sin(\omega t)\hat{\mathbf{y}}]$, and ask what the force of interaction is when averaged over one cycle of the field. This field is at an angle $\phi = \omega t$ to the x axis, so the instantaneous field is $\mathbf{H}_0 = H_0(\cos\phi\hat{\mathbf{x}} + \sin\phi\hat{\mathbf{y}})$. The self-consistent moment of the kth dipole is $\mathbf{m}_k = \mathbf{m}_{x,k}\cos\phi + \mathbf{m}_{y,k}\sin\phi$, where $\mathbf{m}_{x,k}$ is the moment with applied field along $\hat{\mathbf{x}}$. The interaction force is $f_{i,k}(\phi) = f(\mathbf{m}_{x,i}\cos\phi\hat{\mathbf{x}} + \mathbf{m}_{y,i}\sin\phi\hat{\mathbf{y}}, \mathbf{m}_{x,k}\cos\phi + \mathbf{m}_{y,k}\sin\phi)$, or

$$f_{k,i}(\phi) = f_{k,i}(0)\cos^2\phi + f_{k,i}(\pi/2)\sin^2\phi + [f(\mathbf{m}_{x,i},\mathbf{m}_{y,k})$$
$$+ f(\mathbf{m}_{y,i},\mathbf{m}_{x,k})]\cos\phi\sin\phi. \qquad (1)$$

To this force add the value when the applied field is at 90° to ϕ, $f_{k,i}(\phi\pm\pi/2)$. The cross terms cancel, with the result $f_{k,i}(\phi) + f_{k,i}(\phi\pm\pi/2) = f_{k,i}(0) + f_{k,i}(\pi/2)$. The interaction force between a pair of dipoles in an aggregate of dipoles, when summed for two orthogonal fields *applied at separate times*, is thus independent of the angle ϕ. The average interaction force in a rotating field is a simple average of the forces in orthogonal fields,
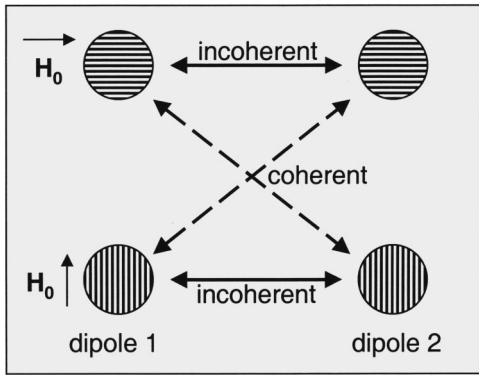
FIG. 2. During 2-d heterodyning there is an oscillation between the coherent and incoherent addition of dipole interactions. Coherent addition occurs when the moment of dipole 1 with the field along the x direction interacts with the moment of dipole 2 with the field along the y direction and vice versa.

$$\tfrac{1}{2} f_{k,i}(0) + \tfrac{1}{2} f_{k,i}(\pi/2) = \tfrac{1}{2} f(\mathbf{m}_{x,i},\mathbf{m}_{x,k}) + \tfrac{1}{2} f(\mathbf{m}_{y,i},\mathbf{m}_{y,k}), \tag{2}$$

so the dipoles are interacting *incoherently* when the x- and y-field components are in quadrature phase. In other words, the dipole moments when the applied field is in the x direction do not interact with the dipole moments when the applied field is in the y direction.

Compare this result to applying the field components in phase, to create an ac field $\mathbf{H}_0 = H_0[\sin(\omega t)\hat{\mathbf{x}} + \sin(\omega t)\hat{\mathbf{y}}]$ at $45°$ to the x axis. In this case the cross terms

$$[f(\mathbf{m}_{x,k},\mathbf{m}_{y,k}) + f(\mathbf{m}_{y,k},\mathbf{m}_{x,k})]\cos(\pi/4)\sin(\pi/4) \tag{3}$$

must be added to Eq. (2) to obtain the correct force. This is a *coherent* interaction between dipoles, Fig. 2. In heterodyned fields there is an oscillation between coherent and incoherent interactions.

2-d heterodyning

To create heterodyning in a biaxial field one adjusts the component frequencies to be sufficiently close that the beat frequency $\Delta\omega$ is slow enough for the particle suspension to

react to it. The field can then be written as $\mathbf{H}_0 = H_0\{\sin[(\omega + \Delta\omega/2)t]\hat{\mathbf{x}} + \sin[(\omega - \Delta\omega/2)t]\hat{\mathbf{y}}\}$ since the relative phase of the two sinusoids is no longer important. Under the conditions where $\Delta\omega \ll \omega$ the sinusoids will oscillate many times before the "relative phase" term $\alpha = \Delta\omega t$ changes, so that over a small time interval the field can be thought of as $\mathbf{H}_0 = H_0[\sin(\omega t + \alpha)\hat{\mathbf{x}} + \sin(\omega t)\hat{\mathbf{y}}]$ within an arbitrary overall phase.

Writing the phase as $\alpha = n\pi/4$, a plot of H_x versus H_y reveals the following sequence: $n=0$ gives a linear (ac) field at $45°$; $n=1$ gives a clockwise elliptical field whose major axis is at $45°$ to the x axis; $n=2$ gives a clockwise rotating field; $n=3$ gives a clockwise elliptical field whose major axis is at $135°$; $n=4$ gives a linear (ac) field at $135°$; $n=5$ gives a counterclockwise elliptical field whose major axis is at $135°$; $n=6$ gives a counterclockwise rotating field; $n=7$ gives a counterclockwise elliptical field whose major axis is at $45°$; and $n=8$ restarts the sequence. This is illustrated in Fig. 3. Intermediate values of n always correspond to elliptical fields at either $45°$ or $135°$ to the x axis. When this heterodyned biaxial field is combined with an orthogonal uniaxial field at a significantly different frequency, an oscillation between a triaxial field and a biaxial field occurs. This is apparent in the simulated structures shown in Fig. 4.

A straightforward generalization of Eq. (1) to arbitrary field component phasing gives the contribution of the field produced by dipole k to the force on dipole i at the time given by $\phi = \omega t$,

$$f_{k,i}(\phi) = f_{k,i}(0)\sin^2(\phi + \alpha) + f_{k,i}(\pi/2)\sin^2\phi$$
$$+ [f(\mathbf{m}_{x,i},\mathbf{m}_{y,k}) + f(\mathbf{m}_{y,i},\mathbf{m}_{x,k})]\sin(\phi + \alpha)\sin\phi. \tag{4}$$

To obtain the average interaction during a single beat of the "carrier" frequency ω we compute the short-time average of Eq. (4),

$$f_{k,i}(\alpha) = \tfrac{1}{2} f_{k,i}(0) + \tfrac{1}{2} f_{k,i}(\pi/2) + [f(\mathbf{m}_{x,i},\mathbf{m}_{y,k})$$
$$+ f(\mathbf{m}_{y,i},\mathbf{m}_{x,k})]\cos(\Delta\omega t). \tag{5}$$
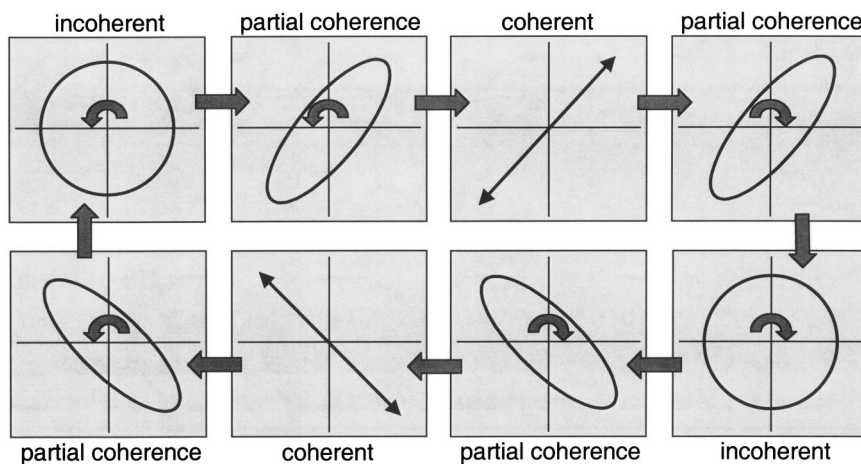
FIG. 3. A sequence of Lissajous loops (plots of H_x vs H_y) during heterodyning. The dipoles interact incoherently when the loop is circular, and interact coherently when the loop collapses to a line.
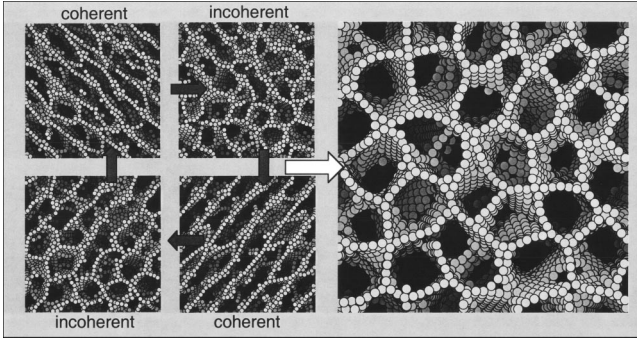
FIG. 4. Series of structures during 2-d heterodyning of a triaxial field. The view is along the uniaxial field, i.e., normal to the heterodyned biaxial field. The periodic formation of sheets occurs when the heterodyned field in the x-y plane becomes linear. This linear ac field combines the uniaxial field to create a pure biaxial field, and sheets form in this field plane. During gelation this produces a honeycomb structure.

This shows that the incoherent force has added to it a coherent cross term that is modulated at the heterodyning beat. In computer simulations of heterodyning one can use a force averaged over the carrier cycle, reducing the computation time by an enormous amount, and eliminating ω as a variable. This is correct to do when structural evolution times are slow compared to $1/\omega$ and fast compared to $1/\Delta\omega$. During gelation there is a crossover where structural evolution times are slow compared to $1/\Delta\omega$, as discussed below.

A time average of the heterodyned interaction force Eq. (5) over a single cycle of the beat frequency recovers the incoherent force in Eq. (2). Thus if the beat is rapid compared to structural organization times the evolution of structure is unaffected by the beat.

3-d heterodyning

In three dimensional heterodyning all three fields beat at a low frequency. It is not easy to envision the dynamically changing Lissajou loop in this case. To understand 3-d heterodyning it is useful to write Eq. (5) in the form (dropping the subscripts i,k) $f(t) = \frac{1}{2}f_{xx} + \frac{1}{2}f_{yy} + f_{xy}\cos(\Delta\omega_{xy}t)$. In this simplified notation f_{xx} refers to the force between dipoles in a uniaxial field of amplitude H_0 applied along the x axis, whereas $f_{xy} = f_{yx}$ is the cross term. To obtain the general case define the matrix $\mathbf{F}$, such that $\mathbf{F}_{xy} = f_{xy}$. Defining the symmetric heterodyning matrix

$$\Omega = \begin{bmatrix} 1 & \cos(\Delta\omega_{xy}t) & \cos(\Delta\omega_{xz}t) \\ \cos(\Delta\omega_{xy}t) & 1 & \cos(\Delta\omega_{yz}t) \\ \cos(\Delta\omega_{xz}t) & \cos(\Delta\omega_{yz}t) & 1 \end{bmatrix}. \quad (6)$$

gives the compact expression $f = \frac{1}{2}\Omega\mathbf{F}$ for the force averaged over the carrier frequency. One beat frequency is the sum of the other two, so there are only two independent beat frequencies. If there is a definite phase relation between the fields, it is simple to introduce these phases into the heterodyning matrix. Equation (6) is the force used in our heterodyning simulations.
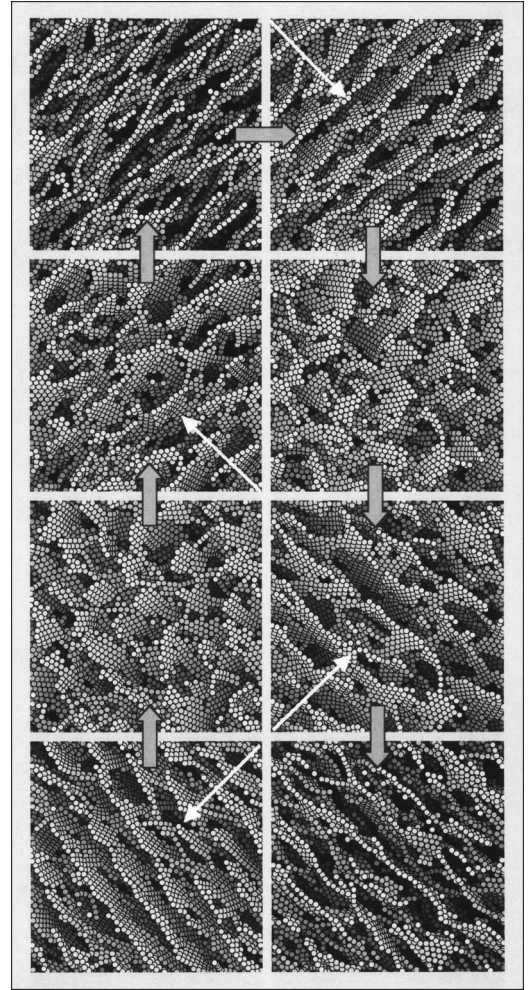
FIG. 5. Series of structures during 3-d heterodyning of a triaxial field. Sheets form normal to the body diagonals of a cube (white arrows) whose faces are normal to the cylindrical axes of the Helmholtz coils.

Three dimensional heterodyning creates a particle dynamics wherein sheets appear in an apparently unpredictable manner normal to the four body diagonals of a cube whose faces are normal to the field components, especially when the beat frequencies are related to each other by a ratio of large integers. The 3-d heterodyning simulation sequence in Fig. 5 gives some idea of the complex dynamics.

Gelation

In a gelling liquid the viscosity diverges to infinity at the gel point. Because of this divergence, a heterodyned particle suspension will no longer be able to couple to the beat at some time before gelation, which has interesting and important effects on structure. According to dynamical scaling theory this viscosity divergence is $\eta \approx |t - t_{\mathrm{gel}}|^{-4/3}$ [18]. One approach to gelation is to incorporate this result into a heterodyning simulation. The disadvantage of having the Stokes drag diverge is poor computational efficiency—after a time the particles essentially quit moving. It is more efficient to chirp the heterodyne frequencies, and the manner in which
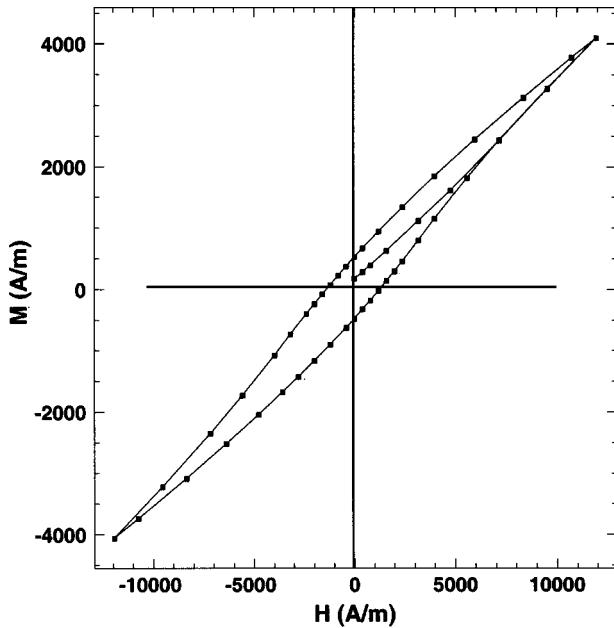
FIG. 6. Magnetization loop for a 6.8-vol % Ni composite shows a remanence of $\approx 13\%$ of the maximum M, giving a residual dipolar interaction only 1.7% of the maximum.

this is done is really not too critical. We ran simulations for 100 dimensionless time units, and used $\Delta\omega = \Delta\omega_0/(1 - t/105)$ as the chirp function, with the initial beat frequencies close to one reciprocal dimensionless time unit. It is remarkable to us that heterodyning during gelation is so effective in producing particle foamlike structures that appear to be very close to minimum magnetostatic energy structures in a triaxial magnetic field.

EXPERIMENTAL RESULTS

Preliminaries

Because these experiments are done in oscillating fields it is important that the particles do not exhibit a strong frequency-dependent susceptibility over the experimental range of frequencies. Results for the Ni powder show that this is indeed the case, with an imperceptible change in the susceptibility from 1 to 10^3 Hz. It is also important that the particles exhibit very little remanent moment, since this could lead to magnetization lags, sample heating, and other undesirable effects. A minor hysteresis loop at a maximum field of 12×10^3 A/m confirms that this is indeed the case, with the zero-field moment being only 13% of the moment at 12×10^3 A/m, Fig. 6. Because interactions depend on the moment squared, residual interactions are only 1.7% of the maximum at this field. These Ni particles adequately fulfill the requirements of these experiments.

It is helpful in the following to define some conventions. The biaxial field will be in the x-y plane and the uniaxial field along the z axis. The rms components of the biaxial field will always be equal. A field bias will refer to the relative magnitude of the rms value of the uniaxial field to that of one component of the biaxial field, a positive bias meaning the uniaxial field is greater. When the composites are anisotropic, the specific susceptibilities will be presented as $(\chi_{xy}/\phi, \chi_z/\phi)$, where ϕ is the particle volume fraction.

The susceptibilities are proportional to the energy of these structures in the magnetic field. For a field applied along the z axis the specific susceptibility of the composite is $\chi/\phi = \chi_p \langle \mathbf{H}_{\text{loc}} \cdot \hat{\mathbf{z}} \rangle / H_0$. The average energy of a dipole is $U = -\frac{1}{2}\mu_0 m_0 \langle \mathbf{H}_{\text{loc}} \cdot \hat{\mathbf{z}} \rangle$, where U is the change in free energy when a dipole is brought into the applied field and moved into its final position in the composite. Normalizing by the magnitude of the energy of an isolated dipole brought into the uniform field, $\frac{1}{2}\mu_0 m_0 H_0$, gives the dimensionless energy $\bar{u} = -\langle \mathbf{H}_{\text{loc}} \cdot \hat{\mathbf{z}} \rangle / H_0$, and $\chi = -3\beta\phi\bar{u}$.

Isotropic samples

The goal of this paper is to demonstrate that it is possible to organize the particles in a suspension to improve its susceptibility along all directions. Because the energy is related to the susceptibilities, structuring in a balanced triaxial field would not occur were this not the case, because there would be no magnetostatic energy gradient to drive particle motions. Experiments have shown that structuring does indeed occur, so the remaining issue is quantitative: How great is the increase?

Control

A random particle composite containing 6.8% Ni was found to have a measured specific susceptibility of 7.1. This is considerably higher than the prediction of Maxwell-Garnet theory, $\chi/\phi = 3\beta/(1 - \beta\phi)$, which gives $\chi/\phi = 3.33$ for $\beta = 1$ (although this theory was developed for dielectrics, the magnetic case is isomorphic). Much of this discrepancy is due to the irregular shape of the Ni particles, because to a good approximation the susceptibility of a random composite is determined by the average susceptibility of the particles of which it is composed, where the average particle susceptibility is the arithmetic average over three orthogonal directions. For ellipsoids composed of a high susceptibility material, the susceptibility along any principal axis is given by the inverse demagnetization factor along that axis, $1/n_w$. Averaging this over three directions gives the single-particle value $\chi/\phi = (\frac{1}{3})(1/n_x + 1/n_y + 1/n_z)$. Demagnetization factors obey the sum rule $n_x + n_y + n_z = 1$, so χ/ϕ is minimized for a sphere, with $n_w = \frac{1}{3}$. Ellipsoids can have a much larger value for χ/ϕ. For particles with extreme aspect ratios this argument will apply only if the permeability of the material of which they are composed is extremely large. Additionally, it is possible that multipolar interactions play a role, but this is doubtful in a random sample at this concentration.

Triaxial field

Structuring a 6.8-vol % sample with a triaxial field of component frequencies (160, 203.7, 180 Hz) gave $\chi/\phi = 8.4$ with rms field amplitudes of 4×10^3 A/m (50 Oe), $\chi/\phi = 11.0$ at 8×10^3 A/m, rising to $\chi/\phi = 13.0$ at 12×10^3 A/m. This latter value constitutes an 83% increase over that of the random sample. Subjecting the sample to 2-d heterodyning with a beat frequency of up to 0.4 Hz (203.3,

203.7, 250 Hz) gave values as large as $\chi/\phi = 13.8$ at 8×10^3 A/m, and 14.4 at 12×10^3 A/m. This is more than a twofold enhancement in the susceptibility, which is quite significant for properties such as magnetostriction, which depend on the square of the susceptibility. 3D heterodyning (203.3, 203.7, 204.2 Hz) gave $\chi/\phi = 13.8$ at 8×10^3 A/m and 13.9 at 12×10^3 A/m.

Samples were also run at higher volume fractions, where the specific susceptibilities are higher due to the increased Lorentz cavity field. A random composite at 20.0 vol % gave $\chi/\phi = 9.7$, and a sample 3-d heterodyned and amplitude modulated gave $\chi/\phi = 15.2$, a 57% increase. In this case the rms field was 8×10^3 A/m, the heterodyne beats were 0.1 and 0.2 Hz, and one field component was amplitude modulated at 1.2 Hz. At 30 vol % a random sample gave $\chi/\phi = 11.8$, a 2-d heterodyned sample at 8×10^3 A/m gave 15.8, and a 3-d heterodyned sample at the same field gave 17.5, a 48% increase over random. Amplitude modulation yielded a comparable result. The benefits of using fields to structure particles diminish somewhat at higher particle volume fractions, but in all cases triaxial magnetic fields significantly improve the composite susceptibility. Other properties, such as the electrical and thermal conductivity, are increased much more and a detailed investigation of the electrical conductivity is in progress.

Anisotropic composites

It is of some interest to use triaxial magnetic fields to create anisotropic composites, to determine whether the susceptibilities of such materials can exceed that of chains formed in a uniaxial field or sheets formed in a biaxial field. Anisotropic composites can be generated by a variety of techniques.

Chains and sheets

We have previously reported measurements of the magnetic properties of particle chains and sheets of Fe carbonyl particles, but to provide an accurate comparison to the more complex structures generated here, we remade these composites with Ni particles. FSC's of chains were made at 6.8 vol % using rms fields of 4×10^3, 8×10^3, and 12×10^3 A/m. Perpendicular to the chains the susceptibilities were nearly invariant to the applied field, with $\chi/\phi = 5.7$, significantly below that of a random composite. Parallel to the chains the susceptibility increased with the applied field, giving the progression $\chi/\phi = 14.9$, 16.9, 17.2. Although the single axis value is high, even at the highest field the specific susceptibility averaged over three directions was only 9.6.

Sheets at 6.8 vol % were run at the same three field amplitudes and at coil frequencies of 160 and 203.7 Hz. Normal to the sheets a strong suppression was observed, $\chi/\phi = 4.3$, 5.0, 4.9, and in the plane of the sheets a significant enhancement was observed, with $\chi/\phi = 12.0$, 13.6, 14.7. Even at the highest field the average specific susceptibility is only 11.4, well below that obtained with triaxial fields.

2-d heterodyning

Samples at 6.8 vol % were made with a heterodyne beat of 0.4 Hz. With the rms field amplitudes balanced at 12
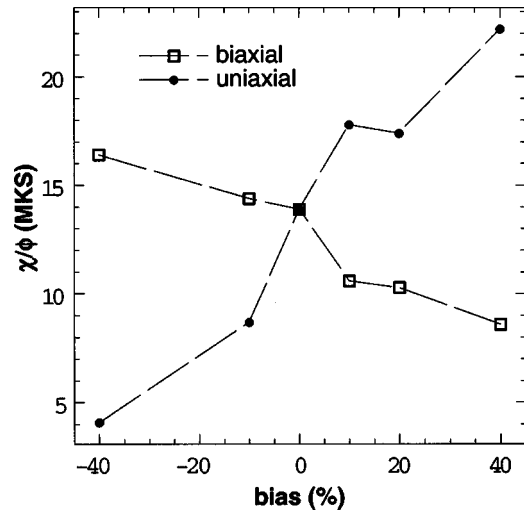
FIG. 7. The biaxial and uniaxial specific susceptibilities for 6.8-vol % Ni composites structured in biased triaxial fields. Even small biases create significant anisotropies.

$\times 10^3$ A/m we recall this gave an average of $\chi/\phi = 14.4$. A $+25\%$ bias induces a significant anisotropy, with $\chi/\phi = (11.7, 20.1)$ for an average of 14.5. The uniaxial susceptibility is greater than that obtained for chains, and the biaxial value is considerably greater. A -25% bias gives $\chi/\phi = (16.6, 4.4)$ and an average value of 12.5, which is much better than obtained in a biaxial field. The susceptibility anisotropy is nearly 4.

At a reduced field of 8×10^3 A/m and a beat frequency of 0.2 Hz an isotropic 6.8 vol % sample gave $\chi/\phi = 13.0$. A $+25\%$ bias gave $\chi/\phi = (9.8, 18.7)$, for an average of 12.8 and a -25% bias gave $(15.1, 8.0)$ for an average of 11.9. The negative bias consistently reduces the average susceptibility.

3-d heterodyning

Samples at the same particle loading were made with 3-d heterodyne beats of 0.4 and 0.5 Hz. With balanced rms field amplitudes of 12×10^3 A/m we recall this gave an average of $\chi/\phi = 13.8$. A $+25\%$ bias gives $\chi/\phi = (10.3, 23.1)$ for an average of 14.6. A -25% bias gives $(16.1, 3.9)$, for an average of 12.0. The value 23.1 is the largest we would measure and is more than $3\times$ that of the random sample. These biased 3-d heterodyning experiments were repeated at a lower rms field of 8×10^3 A/m and at beat frequencies 0.1, 0.2 Hz. Results were similar, but the effects reduced, a $+25\%$ bias giving $\chi/\phi = (10.3, 16.0)$ and a -25% bias giving $(16.7, 5.7)$.

It became apparent that even small field imbalances could lead to significant anisotropies in the composites. To investigate this a series of 6.8-vol % samples were made with biaxial rms amplitudes of 12×10^3 A/m and biases from -40% to $+40\%$. The heterodyne beats were 0.9 and 1.0 Hz. The results in Fig. 7 show that the uniaxial susceptibility doubles from a -10% to a $+10\%$ bias although the average susceptibility is only slightly affected. Because of this it is difficult to make highly isotropic samples at this low particle concentration. For example, with no intentional bias the
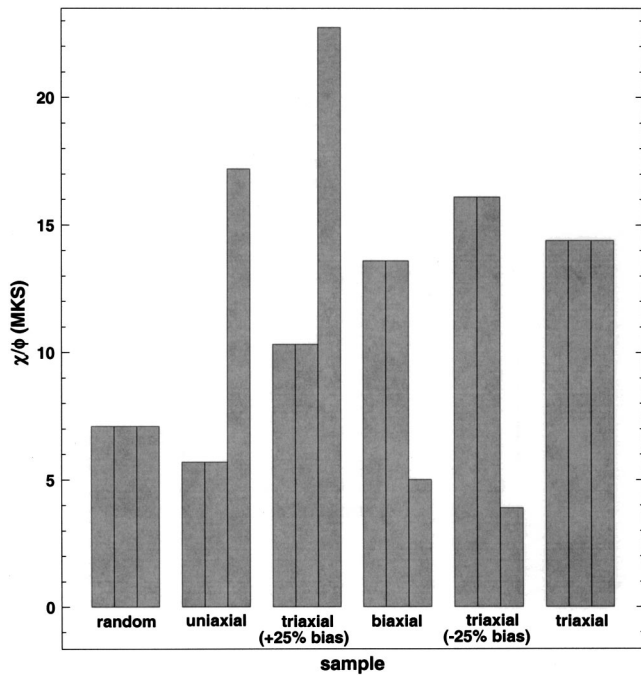
FIG. 8. A comparison between the susceptibilities of 6.8-vol % FSC's made in uniaxial, biaxial, and triaxial fields demonstrates the advantages of using triaxial fields.

three principal susceptibilities can vary $\pm 10\%$ from the average.

The comparison in Fig. 8 between chains, sheets, and various triaxial composites summarizes the improvements triaxial fields enable. The specific susceptibility can be reduced to as little as 3.9 or increased to as much as 23.1. In Fig. 9 are shown the magnetization curves for a random sample, and the lowest and highest susceptibilities we were
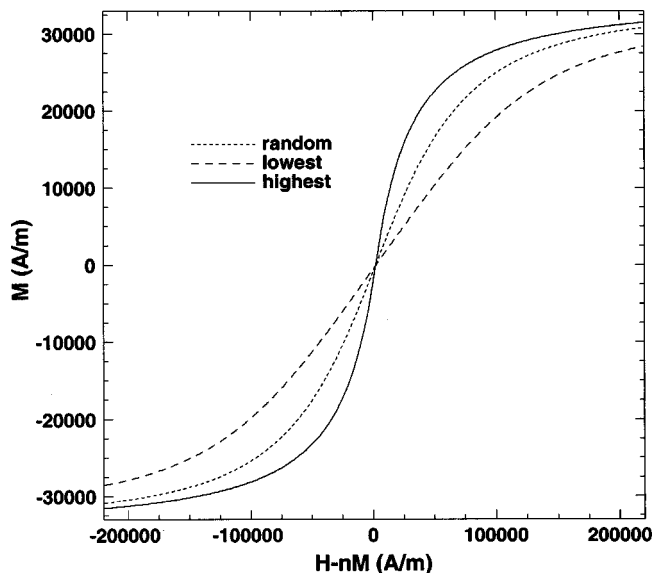
FIG. 9. Full magnetization curves for a random composite at 6.8 vol % are compared to FSC's that had the greatest enhancement and supression, this showing the full range of modification we were able to achieve.

able to produce, all plotted against the internal field.

Higher loadings

At higher particle concentrations the same trends hold, but the effects are reduced. A study of 2-d heterodyning at 20 vol % was done with a beat frequency of 0.4 Hz and at rms fields of 12×10^3 A/m. Under balanced conditions this gave $\chi / \phi = 15.9$. With a $+25\%$ bias the values become (14.5, 19.1) for an average of 16.0, and a -25% bias gives (15.7, 9.9). The average susceptibility is only 13% smaller for the negative bias sample, and the anisotropies are considerably smaller than those at 6.8 vol %.

3-d heterodyning with beats at 0.4, 0.5 Hz gave similar effects at the same field amplitudes. In a balanced triaxial field the specific susceptibility was 16.5. With a $+25\%$ bias the specific susceptibilities are (15.3, 19.7), averaging 16.7, whereas a -25% bias gives (16.1, 9.0). The average susceptibility is 17% smaller for the negative bias case. Amplitude modulation proved to have little additional effect, giving (14.3, 18.5) for a $+25\%$ bias. At 30.0 vol % the structures did not become appreciably anisotropic with field biases of $\pm 25\%$, though biasing experiments were tried with 2- and 3-d heterodyning and amplitude modulated 3-d heterodyning.

Memory effects

Particle sheet structures are low in magnetostatic energy in a balanced triaxial field. So the issue arose as to whether such structures, once formed, would appreciably reorganize in a triaxial field. To test this we subjected a 6.8% suspension to a biaxial field for 20 s, then turned on the uniaxial field. All rms field amplitudes were 8000 A/m and field frequencies were (150, 203.7, 180 Hz). The result was a composite with significant anisotropy, $\chi / \phi = (13.7, 6.8)$. These values are quite close to the values (13.6, 5.0) for sheets formed at the same field amplitudes, indicating strong memory effects under these effectively athermal conditions.

SIMULATION RESULTS

There are two principal issues that simulations can address: the sensitivity of structure to field biasing, and the efficacy of heterodyning in achieving a structure that minimizes the magnetostatic energy and maximizes the average susceptibility. Before discussing these issues we will investigate composites produced athermally.

Athermal

Athermal structures were evolved over 25 dimensionless time units. A random composite at 10 vol % gives $\chi / \phi = 3.4$, in accord with the 3.33 prediction of Maxwell-Garnet theory. Chains produced from a uniaxial field give $\chi / \phi = (3.0, 8.3)$ and sheets give (8.1, 1.7). A triaxial field gives a structure that looks like a gel of chains with $\chi / \phi = 4.8$. The average specific susceptibility of this particle gel is comparable to that of the chains, but significantly lower than that of the sheets, 6.0. This is apparently because the particle gel
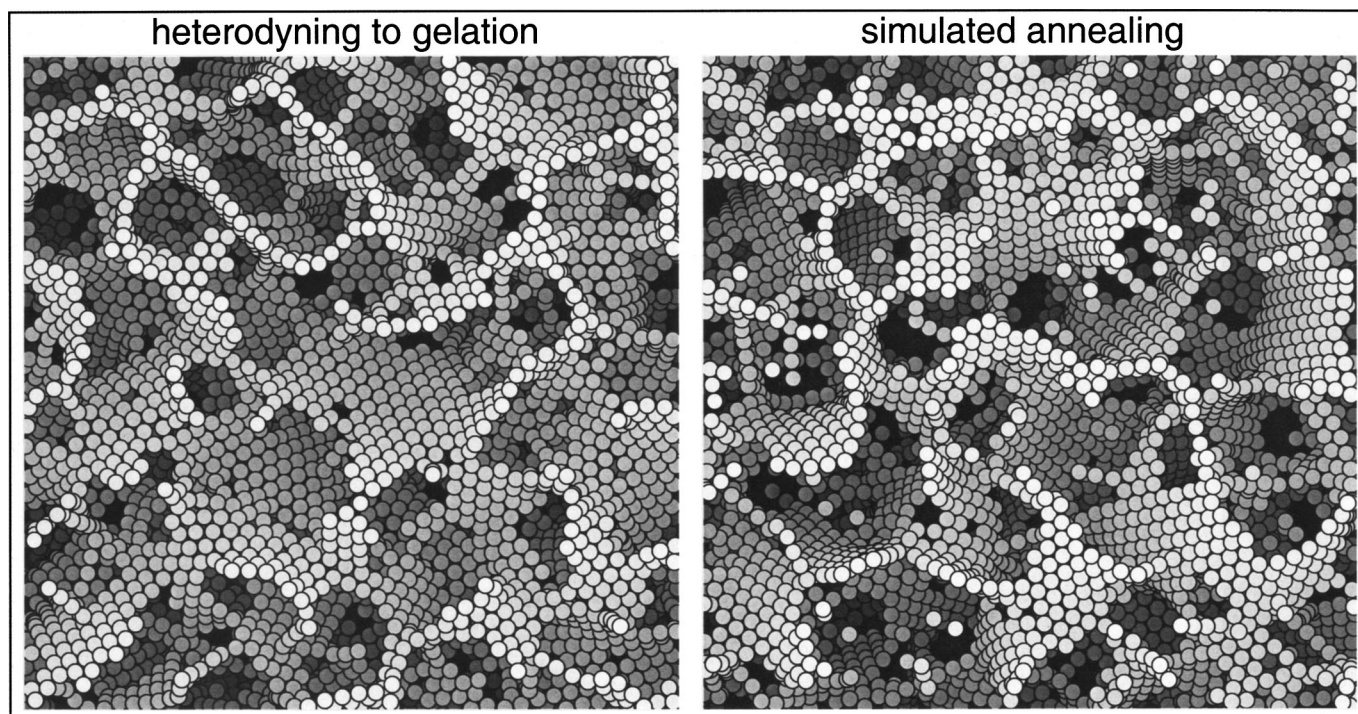
FIG. 10. A composite produced by athermal 3-d heterodyning is statistically indistinguishable from one produced by simulated annealing.

structure is trapped in a deep local minima, like a glass. Simulated annealing should give improved results.

Thermal

A 10-vol % thermal simulation in a biaxial field gives results nearly indistinguishable from the athermal simulation, $\chi/\phi = (8.0, 1.8)$, and likewise for chains (3.0, 8.1). In our previous paper on triaxial fields we found that a large single sheet is in fact a very low energy structure [2]. The specific susceptibilities of a single infinite sheet are (9.7, 1.3), averaging 6.9, so the thermal biaxial structure is close to this bound. The simulated "chain" structure is actually composed of columns and is less anisotropic than an infinite chain, where $\chi/\phi = (2.3, 7.5)$.

In a triaxial field temperature has a dramatic effect, producing a particle foam with $\chi/\phi = 5.5$. This number is still not as high as the biaxial average of 6.0, which must be due to the existence of many local minima on the balanced triaxial field energy surface. Still, these results lend support to the memory effect reported above, where the biaxial field was turned on 20 s before the uniaxial field, leaving a sheetlike structure.

In our experiments the Brownian forces are small compared to the dipolar forces. This is unavoidable because turning down the applied field to the point where Brownian forces are comparable would quickly result in particle sedimentation. Our solution to this is to attempt to mimic the effects of Brownian motion through heterodyning. How well does this coherent effect actually work?

Heterodyning

Heterodyning proved to be effective in increasing the composite susceptibility. Simulations indicate that 3-d het-

erodyning produces the same particle foam structure as simulated annealing, Fig. 10, and yields the same specific susceptibility of 5.5. The manner in which the susceptibility evolves is curious, Fig. 11, because of the pronounced oscillations and the minimum at intermediate times. At early times, when the resin viscosity is still low, the suspension
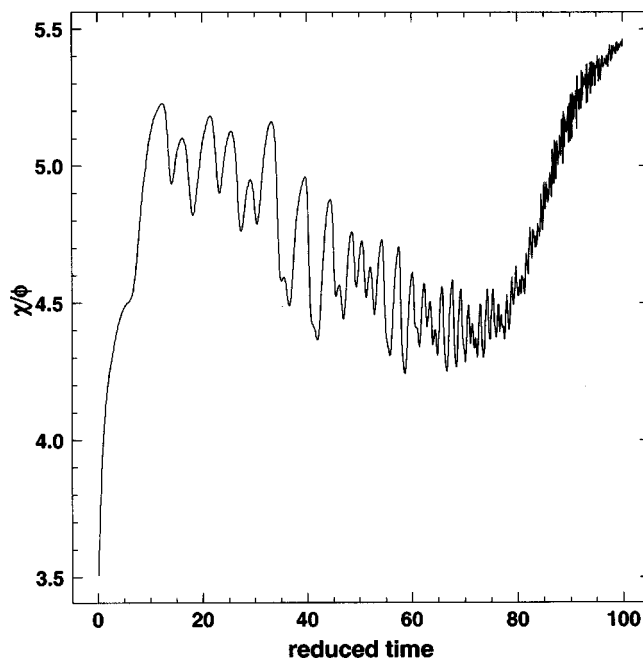
FIG. 11. The average susceptibility as a function of time for a simulated composite produced by 3-d heterodyning during gelation. Note that the fluctuations diminish near the gel point, and the sample becomes isotropic as the average susceptibility increases.
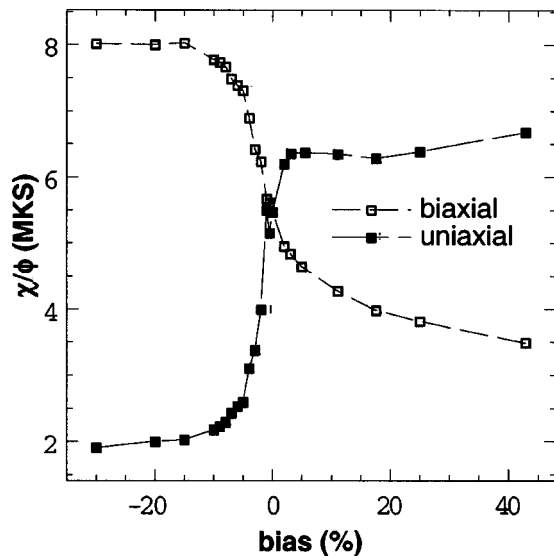
FIG. 12. The biaxial and uniaxial specific susceptibilities for 10.0 vol % created by simulated annealing in biased triaxial fields. A negative bias of a few percent can create an extremely large anisotropy.

dynamics consists of parallel sheets that form normal to one of the four body diagonals of a cube, then fragment and reorient normal to another body diagonal. As the resin viscosity increases, the sheets break into smaller fragments and the average susceptibility actually decreases. Finally, at very large resin viscosities these fragments start to fibrillate into some mean position, forming an isotropic particle foam that is a high susceptibility, low free-energy state. We find it remarkable that such highly correlated motions achieve the effect of thermal motions in these composites.

Unlike Brownian motion, heterodyning can be anisotropic. Simulations of 2-d heterodyning result in an oriented particle foam with the cavities aligned normal to the heterodyning plane, Fig. 4, as in the actual structure. This structure has significant susceptibility anisotropy, with $\chi/\phi = (4.34, 8.12)$, and a high average susceptibility of 5.60. Experiments give a much lower anisotropy, with $\chi/\phi = (13.6, 15.9)$. We believe the roughness of the real particles tends to lock the particles into structures that cannot fully relax to their minimum energy, even with the assistance of heterodyning. 2-d heterodyning on the Ni suspensions only leads to a well-defined honeycomb structure when a positive bias is introduced.

Biased triaxial field

A plot of the uniaxial and biaxial susceptibilities as a function of bias is shown in Fig. 12, these results obtained by simulated annealing. Most striking is the dramatic effect even a small negative bias has, in qualitative agreement with the experimental data in Fig. 7. The quantitative effects are even greater than observed in the experiments, again likely due to particle roughness and the fact that Brownian motion is negligible for the Ni particles, both of which lead to trap-
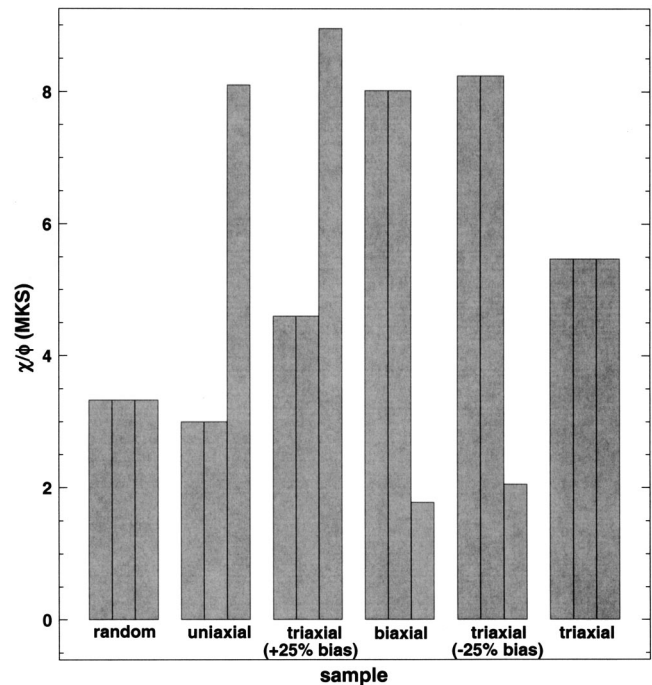
FIG. 13. A comparison between the susceptibilities of simulated 10-vol % FSC's made in uniaxial, biaxial, and triaxial fields. The trends are similar to the real data in Fig. 8, but one real discrepancy is the larger-than-expected values in the biaxial field, and in the negatively biased triaxial field.

ping into metastable states. The simulated composites easily form sheet structures with negative bias, because sheets are very low in energy.

Biased heterodyning

Biased 2-d heterodyning studies were conducted at 20-vol % particles, to keep the cell size small enough to obtain good statistics. For comparison, at this loading a random composite gives $\chi/\phi = 3.8$, simulated annealing of chains gives (3.6, 8.3), sheets give (9.6, 1.9), and a triaxial field gives 6.7. As in the 10-vol % case, 2-d heterodyning gives an average specific susceptibility comparable to simulated annealing, 7.0, but with significant anisotropy (5.8, 9.2). A bias of -25% reverses this anisotropy, (8.2, 4.0), and a bias of $+25\%$ increases the anisotropy slightly to (5.8, 10.0).

Studies of biased 3-d heterodyning were conducted at 10 vol %. In comparison to the unbiased specific susceptibility of 5.4, a $+25\%$ bias gives (4.6, 8.1) for an average of 5.8, and a -25% bias gives (8.2, 2.1) with an average of 6.2. These are the most extreme simulation values we obtained. The summary of key simulation results in Fig. 13 can be compared to the experimental summary in Fig. 8.

DISCUSSION

In a previous paper [1] we developed a self-consistent treatment of the susceptibility based on a mean-field assumption, using the method of Lorentz. It is of interest to reexamine this treatment to understand why it is an inaccurate approximation for triaxial composites. In the method of

Lorentz the local field is broken into three contributions: the applied field, the field due to the nearby dipoles in a suitably chosen cavity, and the cavity field. We will examine the case where the applied field is along the z axis.

Critique of mean-field theory

Recall that the field produced at a relative position $\mathbf{r}$ by a particle of dipole moment $\mathbf{m}$ is $\mathbf{H}=[3(\mathbf{m}\cdot\hat{\mathbf{r}})\hat{\mathbf{r}}-\mathbf{m}]/(4\pi r^3)$. When a field is applied along the z axis, the dipoles will magnetize in a complex way. A key approximation we made in our previous paper is that the off-axis components of the dipole moments are not important in determining the local field, so that in the self-consistent treatment of the moments we set $m_x=m_y=0$. With this approximation the nearby dipole sum over a spherical cavity is

$$\mathbf{H}_{\mathrm{dip},j}=\frac{1}{2\pi}\sum_i m_{z,i}\frac{P_2(\cos\theta_{z,ij})}{r_{ij}^3} \qquad (7)$$

and the dipole field is strictly aligned with the z axis. Here $P_2(x)=(3x^2-1)/2$ is the second Legendre polynomial and $\theta_{z,ij}$ is the angle the line of centers between the ith and jth dipoles make to the z axis. For this sum to converge, the cavity must be large compared to the internal structural scale of the composite.

Is this *aligned dipole approximation* good? For a 30-vol % random composite this incurs an acceptable -4.7% error. For 30-vol % chains and sheets the error is -1.5%, which is quite good. But for a 30-vol % thermally annealed triaxial composite the error is -24.4%, making this approximation unacceptable. To emphasize this point, for the random composite $\chi/\phi=4.29$, for the triaxial FSC the exact value is much higher, 7.42, but using the aligned dipole approximation gives 5.61, so nearly all of the increase due to triaxial structuring is missed with this approximation.

Add to the aligned dipole approximation the *equivalent site approximation* and the entire triaxial field effect is missed. Assuming that there are no space-dependent correlations between the dipole moments in the cavity and their position, then $\mathbf{m}_i$ can be factored out to give

$$\mathbf{H}_{\mathrm{dip},j}=\frac{-\langle m_z\rangle}{2\pi a^3}\psi_{z,j}\hat{\mathbf{z}}$$

$$\text{where}\quad \psi_{z,j}=-\sum_i\left(\frac{a}{r_{ij}}\right)^3 P_2(\cos\theta_{z,ij}). \qquad (8)$$

As a consequence of the law of cosines the quantity $\psi_{z,j}$ follows the sum rule $\psi_{x,j}+\psi_{y,j}+\psi_{z,j}=0$. In the equivalent site approximation we assume that for each site the $\psi_{w,j}$ are to a good approximation independent of j.

The field for a spherical Lorentz cavity is $\mathbf{H}_{\mathrm{cav}}=\frac{1}{3}\mathbf{M}=(\langle m_z\rangle/4\pi a^3)\phi\hat{\mathbf{z}}$, where the composite magnetization density is $\mathbf{M}=\langle\mathbf{m}\rangle/v$ with $v=4\pi a^3/(3\phi)$ the volume of composite per dipole and ϕ the particle volume fraction. To compute the local field of the jth dipole substitute the appropriate expressions into $\mathbf{H}_{\mathrm{loc}}=\mathbf{H}_0+\mathbf{H}_{\mathrm{cav}}+\mathbf{H}_{\mathrm{dip}}$ and use $\langle m_z\rangle=(4\pi a^3/3)\chi_p\langle\mathbf{H}_{\mathrm{loc}}\rangle$ to obtain $\mathbf{H}_{\mathrm{loc},j}=\mathbf{H}_0$

$+\beta(\phi-2\psi_{z,j})\langle\mathbf{H}_{\mathrm{loc}}\rangle$. Ignoring the critical effect of fluctuations by averaging this expression over all of the dipoles gives $\langle\mathbf{H}_{\mathrm{loc}}\rangle=\mathbf{H}_0+\beta(\phi-2\psi_z)\langle\mathbf{H}_{\mathrm{loc}}\rangle$, where as in our previous paper ψ_z denotes the average for this order parameter. The mean local field is then $\langle\mathbf{H}_{\mathrm{loc}}\rangle=\mathbf{H}_0/[1-\beta(\phi-2\psi_z)]$ and the susceptibility along the z axis, defined by $\mathbf{M}=\chi_z\mathbf{H}_0$, is obtained using $\mathbf{M}=3\beta\phi\langle\mathbf{H}_{\mathrm{loc}}\rangle$,

$$\chi_z=\frac{3\beta\phi}{1-\beta(\phi-2\psi_z)}. \qquad (9)$$

The harmonic average susceptibility over three orthogonal directions is $\langle 1/\chi\rangle^{-1}=3\beta\phi/(1-\beta\phi)$ because of the sum rule $\psi_x+\psi_y+\psi_z=0$. Although this expression for the susceptibility works well for random composites, chains, and sheets, it fails utterly for isotropic triaxial composites, predicting no possible increase in the susceptibility beyond that expected for a random composite. In summary, assuming the induced dipoles are aligned with the applied field and equivalent misses the triaxial effect completely.

Domains

It would be of some interest to have a simple, approximate model of the susceptibility of triaxial composites, especially the isotropic particle gels and foams, and the oriented cellular structures. A better description derives from recognizing that these materials consist of coherent domains. Within these domains Eq. (9) should be a good approximation in principal coordinates for a chain or sheet domain where z axis is unique and the x, y axes are equivalent. For isotropic composites domains exist in all orientations, so for the overall composite

$$\langle\chi\rangle=\beta\phi\left[\frac{1}{1-\beta(\phi-2\psi_z)}+\frac{2}{1-\beta(\phi+\psi_z)}\right] \qquad (10)$$

where we have used $\psi_{xy}=-(\frac{1}{2})\psi_z$. This susceptibility has a minimum at $\psi_z=0$, which corresponds to a random composite. At 10-vol % concentration this gives $\langle\chi\rangle/\phi=3.33$ for a random composite. A chainlike domain has $\psi_z\approx-0.246$ at 10 vol % [1], so $\langle\chi\rangle/\phi=4.1$, which can be compared to the athermal simulation value of 4.8. A sheetlike domain at 10 vol % has $\psi_z\approx+0.428$ [1], giving $\langle\chi\rangle/\phi=4.8$, which although smaller than the 5.5 obtained from simulation gives the correct trend. The formation of domains seems to give a qualitative description of how these materials obtain such high isotropic susceptibilities.

The concept of domain formation can be used to relate one set of experimental data to another. At 10 vol % a random sample gave $\langle\chi\rangle/\phi=7.1$. The average susceptibility of a particle chain sample was 9.6 and for sheets this increases to 11.4. Once again these values are lower than that of the corresponding particle gels and foams, but the trends are reasonable.

Biased triaxial samples can be viewed as being formed of oriented sheets. For example, with a positive bias tubelike structures form. In the biaxial plane the susceptibility is then just

$$\langle \chi \rangle = \frac{3}{2} \beta \phi \left[\frac{1}{1 - \beta(\phi - 2\psi_z)} + \frac{1}{1 - \beta(\phi + \psi_z)} \right]$$

and the uniaxial susceptibility is

$$\langle \chi \rangle = \frac{3 \beta \phi}{1 - \beta(\phi + \psi_z)}.$$

At 20 vol % a sheet composite gives $\psi_z \approx +0.393$ [1] which gives $\langle \chi \rangle / \phi = (4.6, \ 7.4)$. The positive biased 2-d heterodyning result at 20 vol % is (5.8, 10.0). Other comparisons can be made, but the important point is that heterodyned triaxial fields tend to make sheetlike structures and the orientation of these sheets can be manipulated by applying small biases. Overall, better comparisons between the simulated triaxial composites and chain and sheet data can be made by using values $\psi_z \approx -0.301$ [1] for a single long chain and $\psi_z \approx +0.69$ [1] for a single sheet, but the comparison is still qualitative.

CONCLUSIONS

We have shown that it is possible to use triaxial magnetic fields to create magnetic isotropic particle composites with susceptibilities that are greatly enhanced over that of random particle composites. This is especially true when heterodyning of the field components is employed, which manages to mimic the effects of Brownian motion. We have also shown that it is possible to use heterodyned triaxial fields to create anisotropic composites with very high susceptibilities in preferred directions. Overall the simulations support the experimental findings, though the experimental values are larger, most probably due to the reduced average demagnetization field associated with the nonspherical particle shape. Some discrepancies between the simulated and real structures remain which are probably due to particle roughness. A simple interpretation of these results is given in terms of the formation of randomly oriented chain and sheet-like domains.

ACKNOWLEDGMENTS

[1] J. E. Martin, E. Venturini, J. Odinek, and R. A. Anderson, Phys. Rev. E **61**, 2818 (1999).

[2] J. E. Martin, R. A. Anderson, and R. L. Williamson, J. Chem. Phys. **118**, 1557 (2003).

[3] J. E. Martin, R. A. Anderson, and C. P. Tigges, J. Chem. Phys. **108**, 7887 (1998).

[4] T. C. Halsey, R. A. Anderson, and J. E. Martin, Int. J. Mod. Phys. B **10**, 3257 (1996).

[5] J. E. Martin, R. A. Anderson, and R. L. Williamson, patent application, ''Method of using triaxial magnetic fields for making particle structures'' (2002).

[6] K. O'Grady, A. Bradbury, J. Popplewell, S. W. Charles, and R. W. Chantrell, J. Magn. Magn. Mater. **49**, 106 (1985).

[7] D. Brugel, M. R. J. Gibbs, and P. T. Squire, J. Appl. Phys. **63**, 4249 (1988).

[8] S. Jin, T. H. Tiefel, and R. Wolfe, IEEE Trans. Magn. **28**, 2211 (1992).

[9] S. Jin, R. C. Sherwood, J. J. Mottine, T. H. Tiefel, R. L. Opila, and J. A. Fulton, J. Appl. Phys. **64**, 6008 (1988).

[10] P. Fabre, R. Ober, M. Veyssie, and V. Cabuil, J. Magn. Magn. Mater. **85**, 77 (1990).

[11] R. Tao and J. M. Sun, Phys. Rev. Lett. **60**, 319 (1992).

[12] J. E. Martin, R. A. Anderson, and C. P. Tigges, J. Chem. Phys. **110**, 4854 (1999).

[13] J. E. Martin and J. P. Wilcoxon (unpublished).

[14] R. A. Anderson and J. E. Martin, Am. J. Phys. **70**, 1194 (2002).

[15] J. R. Reitz and F. J. Milford, *Foundations of Electromagnetic Theory* (Addison-Wesley, Reading, MA, 1967), p. 96.

[16] J. E. Martin, R. A. Anderson, and C. P. Tigges, J. Chem. Phys. **108**, 3765 (1998).

[17] J. R. Reitz and F. J. Milford, Foundations of Electromagnetic Theory (Addison-Wesley, Reading, MA, 1967), pp. 210–214.

[18] J. E. Martin, D. Adolf, and J. P. Wilcoxon, Phys. Rev. Lett. **61**, 2620 (1988).